2013 IEEE Military Communications Conference

# Link Asymmetry in Virtual MISO-based Networks

Haejoon Jung and Mary Ann Weitnauer*
School of Electrical and Computer Engineering, Georgia Institute of Technology, Atlanta, GA 30332-0250, USA
Email: {hjung35, maweit}@gatech.edu

***Abstract*—Cooperative transmission (CT), in which spatially separated wireless nodes collaborate to form a virtual antenna array or virtual multiple-input-single-output (VMISO) link, is an effective technique to enhance the system performance by spatial diversity. In this paper, we study the link asymmetry issue of the VMISO links between two neighboring CT clusters, which can be used to design higher-layer CT algorithms such as routing and medium access control (MAC). While many authors simplify analysis on CT-based networks with *co-located approximation* that ignores disparate path losses in VMISO links by assuming co-located cooperators, this paper studies the impact of disparate path losses on link asymmetry by allowing the relay locations to be random. We identify two main factors of the VMISO link asymmetry, which do not appear in the conventional SISO-based networks: exclusive signal detection only at a single node and path-loss disparity. The link asymmetry level is evaluated by using the correlation and the ratio of two signal powers in the forward and reverse directions, which presents the distinct characteristics of the VMISO links compared to the conventional SISO links. Moreover, the simulation results show how the VMISO link asymmetry changes depending on various system parameters.**

## I. Introduction

Cooperative transmission (CT), in which spatially separated wireless nodes collaborate to form a virtual antenna array, is an effective technique to mitigate multi-path fading by spatial diversity [1], [2]. In CT, by creating a virtual multiple-input-single-output (VMISO) link between multiple transmitters and a single receiver, the receiver benefits from a signal-to-noise-ratio (SNR) advantage through array and diversity gains. In various types of wireless networks such as wireless sensor networks (WSNs), multi-hop wireless networks (MWNs), and mobile ad-hoc networks (MANETs), the SNR advantage of CT can be used to improve higher layer performances such as throughput, energy efficiency, network lifetime [3]–[12].

To deal with network-scale analysis with random topologies, the CT researchers on higher layer either assume very high node density, which is called "*continuum assumption*," as in [3], [4] or simplify the physically separated nodes into a single node with a multiple-antenna array, which is referred to as "*co-located approximation*" as in [10]–[12]. Following the classification of CT network architectures in [13], the continuum assumption is frequently used in the decentralized CT architecture, where all the nodes have the same role, while the co-located approximation appears in the centralized CT architecture with a cluster head that controls the other cooperating nodes in the cluster, which are typically a subset of the one-hop neighbors of the cluster head.

In this paper, we are interested in the link asymmetry of VMISO links in the centralized architecture, which is neglected by co-located assumption in the previous studies. Link asymmetry adversely affects routing in ad hoc networks, because it causes many routing protocols and link-layer schemes (e.g., AODV and CSMA/CA) to work inefficiently [14]. Similarly, many VMISO-based protocols with the centralized cluster architecture such as [10]–[12] require bidirectional links, because such protocols are modified versions of the conventional single-input-single-output (SISO)-based schemes that assume bidirectional link.

In the conventional SISO-based network, link asymmetry that makes unidirectional links is caused by transceiver hardware difference, uneven transmit power control, and noise or other signal propagation phenomena [15]. In this paper, to focus on link asymmetry of the VMISO links that does not appear in the SISO links, we assume these factors are excluded by calibration. Therefore, in case of time-division duplex (TDD), which is more widely used than frequency-division duplex (FDD) for link-layer signaling (e.g., RTS-CTS-DATA-ACK in *IEEE 802.11* [16]), the forward and reverse channels can be assumed to be equal with frequency nonselective block fading [17]. In other words, the forward and reverse channels have the same channel coefficients in the SISO-based networks. On the other hand, the VMISO-based networks inherently suffer from the link asymmetry because each VMISO link consists of multiple SISO links from different transmitters to a single receiver.

Because of the overhead and the implementational complexity of the cooperative reception [18], most of the CT-based protocols let each node at the receive cluster individually decode its own received signal. Therefore, if looking at the forward and reverse VMISO links between two neighboring clusters with the centralized architecture, the cooperative relays in each cluster are only used for transmission, while a cluster head exclusively decodes the received signal from the other cluster. Thus, considering that multiple SISO links make a single VMISO link, the reverse and forward VMISO links have only one common SISO link, which is between the two cluster heads. On the other hand, the other SISO links between the cooperators in one cluster to the cluster head in the other cluster have independent channel characteristics, because cooperative relays in a cluster impact only on the *transmit* channel to the other cluster. In addition, the link asymmetry

*Mary Ann Weitnauer was formerly Mary Ann Ingram.

978-0-7695-5124-1/13 $31.00 © 2013 IEEE
DOI 10.1109/MILCOM.2013.225

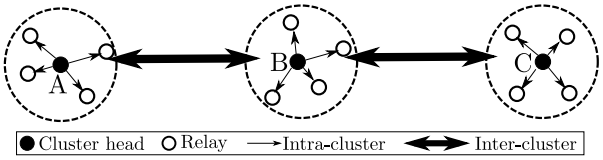


Fig. 1. Logical illustration of a VMISO-based multi-hop network

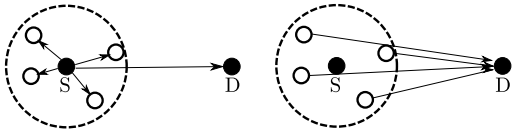


Fig. 2. Two-hop cooperative transmission scenario for each cooperative hop

of the two VMISO links is more severe than the co-located model, because physically separated relays make disparate path losses depending on their locations. Considering these two factors (exclusive signal reception by cluster heads and path-loss disparity), this paper explores the forward-reverse link asymmetry between two CT clusters, while excluding the other factors (e.g., hardware, transmit power, and irregular signal propagation). To our knowledge, there has not been a study about this link asymmetry problem in the VMISO-based networks.

## II. System Model

We consider wireless networks with multiple centralized clusters using CT as shown in Fig. 1, where the large circles with the dashed lines indicate clusters, the black-filled dots, which are labeled with A, B, and C, and the white-filled circles represent three cluster heads and cooperative relays, respectively. First, the intra-cluster cluster communication, which is indicated by the narrow black arrows, is required to recruit cooperating relays and form a virtual array. Then, the inter-cluster transmissions, which are indicated by the thick black arrows, are done in CT using the VMISO links. The CT through the VMISO links in multi-hop networks can have better reliability, higher throughput, and higher energy-efficiency compared to the conventional SISO networks [3]–[12].

Assuming data transmissions from the left to right clusters, a VMISO communication on each cooperative hop consists of two phases as shown in Fig. 2, where the source (or the transmit cluster head), which is labeled with 'S,' first transmits a packet to the destination (or the receive cluster head), which is labeled with 'D', in Phase 1. After that, the multiple relays, which are indicated by the white-filled circles around the source, decode and then forward (DF) using orthogonal channels or space-time codes to the destination in Phase 2 [19]. At the destination, the multiple copies from the source and multiple relays are combined, which provides an SNR advantage.

### A. Network Topology

We consider a multi-cluster network, where the forward and reverse links of each VMISO hop are shown in Fig. 3. In the

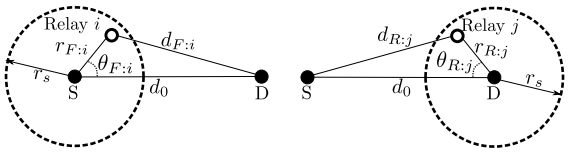


Fig. 3. Network topology model

figure, the distance between the source and destination, which are labeled with 'S' and 'D', respectively, is $d_0$. We assume cooperating relays are uniformly and randomly distributed around the cluster heads (source and destination), in the area of the dashed-line circles with a radius $r_s$ centered at the cluster heads. While $d_0$ indicates the CT transmission range, $r_s$ can be regarded as the maximum SISO range. As in [10]–[12], through the array and diversity gains of CT, we assume the *CT range extension case* with $1.5 \leq d_0/r_s \leq 4$, which was demonstrated in [20]. We note that maximum range extension happens when radios do not decrease their transmit powers when cooperating, and when they transmit using either orthogonal channels or space-time-block-coding, so the link benefits from diversity gain [2].

We assume that $M$ relays in the source cluster and $N$ relays in the destination cluster are independently and identically distributed in the two circles with the radius $r_s$ following the uniform distribution. As shown in Fig. 3, Relay $i$ and Relay $j$ in the source and destination clusters, represented by the white-filled circles, exist at distances of $r_{F:i}$ and $r_{R:j}$ from their cluster heads (source and destination) with angles of $\theta_{F:i}$ and $\theta_{R:j}$ with respect to the line connecting the source and destination, respectively. Also, Relays $i$ and $j$ are $d_{F:i}$ and $d_{R:j}$ away from the other cluster heads respectively, which determines the path losses from the relays to the other cluster heads. It follows that the polar coordinates $(r_{v:w}, \theta_{v:w})$ centered at each cluster head, where $v \in \{F, R\}$ and $w = 1, ..., N$ for $v = F$ or $w = 1, ..., M$ for $v = R$, have the probability distribution functions (PDFs): $f_{r_{v:w}}(r_{v:w}) = \frac{2r_{v:w}}{r_s^2}$ and $f_{\theta_{v:w}}(\theta_{v:w}) = \frac{1}{2\pi}$, where $0 < r_{v:w} \leq r_s$ and $0 \leq \theta_{v:w} \leq 2\pi$, respectively.

### B. Channel Model

We assume mutually independent Rayleigh fading for any links between two nodes in different clusters. The node indices of the two cluster heads (the source and destination) are zero, while the relays have indices $1 \leq i \leq M$ and $1 \leq j \leq N$ for the source and destination clusters, respectively. The complex channel gains of the forward links are denoted by $h_{i,j}$, while the reverse channel gains are denoted by $g_{j,i}$, where $i = 0, ..., M$ and $j = 0, ..., N$ including the communication channels involving the cluster heads. However, we note that only the cluster head in each cluster decodes the signals received from the other cluster in a VMISO network, which means that we only need to consider the channel gains $h_{i,0}$ and $g_{j,0}$ for $i = 0, ..., M$ and $j = 0, ..., N$. For simplicity, we assume unit transmit power for all the nodes. Hence, $\Omega_{F:i} = |h_{i,0}|^2$ and $\Omega_{R:j} = |g_{j,0}|^2$ follow the exponential

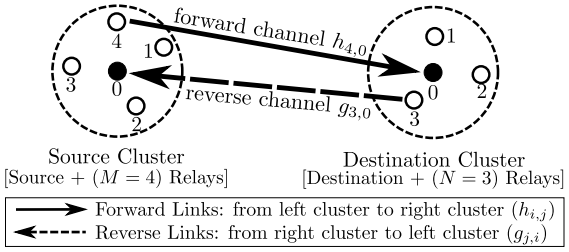


Fig. 4. Illustration of forward and reverse links

distribution with a parameter $\lambda_{F:i} = d_{F:i}^{\alpha}$ or $\lambda_{R:j} = d_{R:j}^{\alpha}$, which is determined by the locations of Nodes $i$ and $j$, with the path loss exponent $\alpha$. The cumulative distribution functions (CDF) of $\Omega_{v:w}$ given $\lambda_{v:w}$ is expressed as

$$F_{\Omega_{v:w}|\lambda_{v:w}}(x) = 1 - e^{-\lambda_{v:w}x}, \tag{1}$$

where $v \in \{F, R\}$ and $w = 1, ..., N$ for $v = F$ or $w = 1, ..., M$ for $v = R$. Also, the conditional mean and variance for given $\lambda_{v:w}$ are $\mathbb{E}\{\Omega_{v:w}|\lambda_{v:w}\} = 1/\lambda_{v:w}$ and $\mathbb{VAR}\{\Omega_{v:w}|\lambda_{v:w}\} = 1/\lambda_{v:w}^2$, respectively.

## III. Correlation of Forward and Reverse Links

### A. Signal Reception Only at the Cluster Head

Without cooperative reception, the centralized CT networks use a single VMISO link in one direction for each hop, because only the receive cluster head decodes, while the cooperative relays are used only for transmission. For a real or virtual MIMO link with $(M + 1)$ transmit antennas and $(N + 1)$ receive antennas, the forward channel gain can be expressed by a $(M + 1) \times (N + 1)$ channel matrix $\mathbf{H}$ that has elements $h_{i,j}$ denoting the channel gain from transmit antenna $i$ to receive antenna $j$. Moreover, the reverse channel matrix $\mathbf{G}$, the dimension of which is $(N + 1) \times (M + 1)$, has elements $g_{j,i}$ that denotes the reverse channel gain from antenna $j$ to $i$. Assuming frequency nonselective block fading, by the reciprocity stated in [17], we can assume $\mathbf{H} = \mathbf{G}^{\mathbf{T}}$, where $\mathbf{T}$ is the matrix transpose. However, a VMISO link uses only a part of the channel matrices $\mathbf{H}$ and $\mathbf{G}$. For example, the forward link channel gains $h_{i,0}$, where $i = 1, ..., M$, are one row of the matrix $\mathbf{H}$. Similarly, the reverse link channel gains $g_{j,0}$, where $j = 1, ..., N$, are one row of the matrix $\mathbf{G}$. Therefore, in general, a VMISO hop has only one common channel gain between the forward and reverse links $h_{0,0} = g_{0,0}$. Assuming unit transmit power for simplicity with maximal ratio combining (MRC), the total received powers at the cluster heads through the forward and reverse links can be represented as $P_F = \sum_{i=0}^{M} \Omega_{F:i}$ and $P_R = \sum_{j=0}^{N} \Omega_{R:j}$, where $\Omega_{F:i} = |h_{i,0}|^2$ and $\Omega_{R:i} = |g_{j,0}|^2$. Because $\Omega_{F:0} = |h_{0,0}|^2 = \Omega_{R:0} = |g_{0,0}|^2$, the correlation coefficient between the two received powers $P_F$ and $P_R$, which is one measure of link asymmetry, is given by

$$\rho = \frac{\mathbb{COV}\{P_F, P_R\}}{\sqrt{\mathbb{VAR}\{P_F\}\,\mathbb{VAR}\{P_R\}}}, \tag{2}$$

where $\mathbb{COV}$ denotes covariance. If excluding the random relay locations by the co-located assumption, which means $d_{F:i} = d_{R:j} = d_0$ for all $i$ and $j$, $\rho$ simplifies to $\frac{1}{\sqrt{(M+1)(N+1)}}$, because the only common component between $P_F$ and $P_R$ is $\Omega_{F,0} = \Omega_{R,0}$, while the other channel power components are independent.

### B. Path-loss Disparity in VMISO

With the co-located approximation, the multiple transmitting nodes in a clusters are assumed to be co-located with the cluster head, which means $\lambda_{v:w} = \lambda = d_0^{\alpha}$ for all $v \in \{F, R\}$, $w = 1, ..., M$ or $N$, as the real antenna array. In this case, the received power $P_v$ at the receiver follows the gamma distribution, the CDF of which is

$$F_{P_v}(y) = 1 - \sum_{w=0}^{L} \frac{\exp(-\lambda y) \cdot (\lambda y)^w}{w!}, \tag{3}$$

assuming unit transmit power and $L$ number of relays (i.e., $L = M$ for $v = F$, while $L = N$ for $v = R$). However, in reality, the relays are physically separated to each other. Therefore, the multiple SISO links between the transmitters (the relays and cluster head of the current cluster) to the receiver (the cluster head in the other cluster) have dissimilar path losses, which means $\lambda_{v:w} \neq \lambda_{v':w'}$ when $v \neq v'$ or $w \neq w'$. For this reason, the received power $P_v$ the follows the hypoexponential distribution, which has the CDF:

$$F_{P_v}(y) = 1 - \sum_{w=0}^{L} A_{v:w} \exp(-\lambda_{v:w} \cdot y), \tag{4}$$

where $A_{v:w} = \prod_{w \neq w'} \frac{\lambda_{v:w'}}{\lambda_{v:w'} - \lambda_{v:w}}$ and $\sum_{w=0}^{L} A_{v:w} = 1$ [21]. Also, the parameters $\lambda_{v:w}$ in this CDF can be simply calculated by $\lambda_{v:w} = d_{v:w}^{\alpha}$, where the PDF of $d_{v:w}$ can be obtained by the variable transformation of $f_{r_{v:w}}(x)$ and $f_{\theta_{v:w}}(x)$ as

$$f_{d_{v:w}}(x) = \frac{x}{\pi r_s^2}\left( \frac{\frac{r_s}{d_0} - \frac{\left(d_0^2 - x^2 + r_s^2\right)}{2d_0 r_s}}{\sqrt{1 - \frac{\left(d_0^2 - x^2 + r_s^2\right)^2}{4d_0^2 r_s^2}}} - \frac{\left(\frac{x}{d_0} - \frac{d_0^2 + x^2 - r_s^2}{2d_0 x}\right)}{\sqrt{1 - \frac{\left(d_0^2 + x^2 - r_s^2\right)^2}{4d_0^2 x^2}}} + 2\arccos\left(\frac{d_0^2 + x^2 - r_s^2}{2d_0 x}\right)\right), \tag{5}$$

for $d_0 - r_s \leq d_{v:w} \leq d_0 + r_s$. Following this PDF, we treat the parameters $\lambda_{v:w}$ as random variables to consider the disparate path losses. In [22], the authors show that the impact of the disparate path losses in a VMISO link on the asymptotic capacity outage in high SNR is equivalent to the degradation by log-normal shadowing, which has the following variance in dB scale:

$$\sigma^2 = \mathbb{VAR}\{10\log_{10}\lambda_{v:w}\} = \frac{c \cdot \alpha^2 \cdot L}{(L+1)^2}\left(\frac{r_s}{d_0}\right)^2, \tag{6}$$

where $c$ is a constant. We can use this $\sigma^2$ as an indicator of the degree of the path-loss disparity. By using this $\sigma^2$, we can estimate how the impact of the path-loss disparity, which can be modeled as log-normal shadowing, changes depending on system parameters such as the path-loss exponent $\alpha$, the distance ratio $r_s/d_0$, and the number of relays $L$.

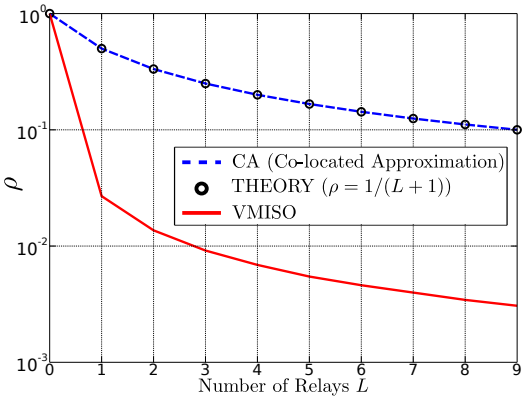


Fig. 5. Correlation coefficient versus number of relays $L$

Fig. 5 shows the impact of the path-loss disparity on $\rho$, where the vertical axis indicates the correlation coefficient $\rho$ in a log scale and the horizontal axis in a linear scale indicates the number of relays $L$, assuming the same number of relays $M = N = L$. In the figure, the blue dotted line, which is labeled with 'CA' in short, indicates $\rho$ obtained from $10^6$ random Rayleigh fading samples for the co-located case, while the circles labeled with 'THEORY' represent the theoretical curve $\rho = 1/(L+1)$. The two (CA and THEORY) graphs show the identical results, as we expected. Lastly, the red line indicates the correlation coefficient $\rho$ of the VMISO links obtained by $10^6$ samples in the presence of path-loss disparity by the random relay locations, when $d_0 = 3$, $r_s = 1$, and $\alpha = 4$. For all the three graphs, $\rho$ decreases as $L$ increases, because each cluster head is the only receiver of a VMISO link. Also, as shown in the figure, the red curve (VMISO) is always smaller than the blue line (CA), which means $P_F$ and $P_R$ become much less correlated by the random relay locations and the corresponding disparate path losses.

## IV. Link Asymmetry Quantified by Power Ratio

As shown in the previous section, the forward and reverse VMISO links become less correlated as the number of relays increases, because of the exclusive reception at the cluster head and the disparate path losses by the random relay topologies. However, from the higher-layer perspective, the received power difference of the two VMISO links, which can be translated into the error rate gap, is more practical than the correlation $\rho$. Therefore, in this section, we use the ratio of the signal powers of the two links as $\eta = \frac{P_R}{P_F}$ to quantify the link asymmetry of the forward and reverse links.

### A. Probability Distribution of $\eta = \frac{P_R}{P_F}$

It is difficult to obtain a closed form expression for the probability distribution of $\eta = \frac{P_R}{P_F}$, because of the disparate path losses and the common elements ($h_{0,0}$ and $g_{0,0}$) of the two VMISO links, which makes $0 < \rho < 1$. Therefore, we can only calculate the probability distribution of $\eta$ by simulation with random samples or numerical computation. On the other hand, in the absence of path-loss disparity and when $h_{0,0}$ and $g_{0,0}$ are also independent (e.g., FDD), the CDF of $\eta = \frac{P_R}{P_F}$ can be obtained by using the outage probability (17) in [23], which is derived to calculate the outage rate determined by signal-to-interference-ratio (SIR) with independent Nakagami signal and Nakagami interference. Applying our system parameters, the CDF of $\eta$ in this case, denoted by $F^*_\eta$, is given by

$$F^*_\eta(x) = \left(1 + \frac{1}{x}\right)^{1-M-N} \cdot \sum_{k=0}^{N-1} \binom{M+N-1}{k} \left(\frac{1}{x}\right)^k. \tag{7}$$

Because the true CDF $F_\eta(x)$ without any approximation, which includes the path-loss disparity and the common channel elements $h_{0,0} = g_{0,0}$, does not give a closed form, the CDF $F^*_\eta(x)$ in (7) can be used to estimate the degree of the link asymmetry, when path-loss disparity is small enough (i.e., $\sigma^2$ in (6) is small) with large $M$ and $N$ (i.e., $\rho$ in (2) is small).

Figs. 6 (a) and (b) show the CDFs $F_\eta(x)$ with the same number of relays ($M = N = 3$) and different number of relays ($M = 5$ and $N = 3$), respectively, when $d_0 = 2$, $r_s = 1$, and $\alpha = 4$. In the figures, the x-axis indicates the ratio $\eta = \frac{P_R}{P_F}$ in a log scale, while the y-axis is the corresponding cumulative probability in a linear scale. In each figure, the black circles labeled with 'CA-indp' in short represent the theoretical CDF in (7) that ignores the common SISO link between the two cluster heads (i.e., $h_{0,0}$ and $g_{0,0}$ are assumed to be independent) in the absence of the path-loss disparity. Moreover, the blue dotted line labeled with 'CA' and red solid line labeled with 'VMISO' indicate the CDF of the co-located approximation and the true VMISO CDF, respectively. Because $F_\eta(x) = \Pr[\eta = \frac{P_R}{P_F} \le x]$, $F_\eta(x) = \Pr[P_R \le x \cdot P_F]$, while $1 - F_\eta(x) = \Pr[P_R > x \cdot P_F]$. Therefore, as the length of the left and right tails increase, an extreme case with a very small or large ratio $\eta$ becomes more likely, which means the link asymmetry of the two VMISO links gets more severe. With this interpretation, the true VMISO curve indicated by the red solid line is more asymmetric than the co-located approximation indicated by the blue dotted line in both figures. Moreover, the black circles, which represent $F^*_\eta(x)$ in (7), indicate show slightly more asymmetric links with the longer tails than the blue curve, because the approximate CDF $F^*_\eta(x)$ assumes that $h_{0,0}$ and $g_{0,0}$ are independent.

If comparing the two figures, all the three graphs in Fig. 6(a) are symmetric about the point $(x, y) = (1, 0.5)$, while in Fig. 6(b) $F_\eta(1) < 0.5$ for all the three curves, which means $\mathbb{E}\{\eta\} < 1$. In other words, statistically $P_F > P_R$ in Fig. 6(b), because the source cluster has more number of relays than the destination cluster. In contrast, in Fig. 6(a), all the three curves satisfy $F_\eta(x) = 1 - F_\eta(1/x)$ by the symmetry about the mean point $(x, y) = (1, 0.5)$. Therefore, for more balanced powers in the both directions, the clusters in multi-hop networks should use the same number of relays. In fact, the authors in [10] propose that all the clusters on a multi-hop CT-based route have to use the same number of nodes to avoid the link asymmetry for their link-layer algorithm, which is a modified version of *IEEE 802.11* MAC. However, the use of a fixed number of nodes cannot completely solve the link asymmetry issue caused by the inherent characteristics of the VMISO communication, which is ignored in [10], as we can see the

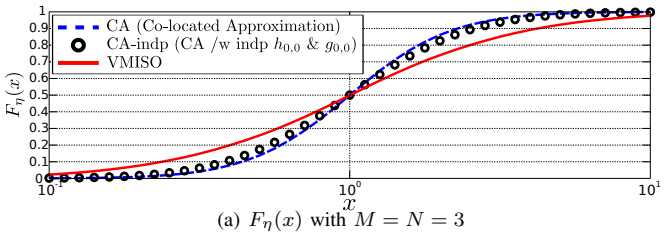


(a) $F_\eta(x)$ with $M = N = 3$

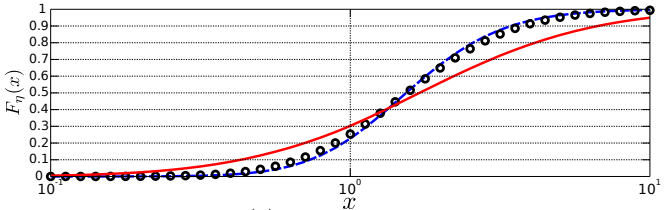


(b) $F_\eta(x)$ with $M = 5$ and $N = 3$

Fig. 6. Two CDFs of $\eta = \frac{P_R}{P_F}$ with $d_0 = 2$, $r_s = 1$, and $\alpha = 4$

long tails in Fig.6(a).

### B. Parametric Study

In this section, we observe the variation in the VMISO link asymmetry depending on the three system parameters: the distance ratio $d_0/r_s$, the path-loss exponent $\alpha$, and the number of relays $L$. We assume the same number of relays for the both clusters $M = N = L$ as a prerequisite to minimize asymmetry compared to the case with $M \neq N$. To measure the degree of the link asymmetry, we look at the probability $p_{2X}$ that the difference of the two powers, $P_F$ and $P_R$, is greater than or equal to 3dB. This probability $p_{2X}$ can be expressed using $F_\eta(x)$ by its symmetry as

$$p_{2X} = \Pr[P_F \geq 2P_R] + \Pr[P_R \geq 2P_F] = 2 \cdot F_\eta(1/2). \quad (8)$$

In the simulation results in Figs. 7, 8, and 9, there are four graphs in each figure: the co-located approximation (the blue dotted line), the theoretical curve assuming independent $h_{0,0}$ and $g_{0,0}$ in (7) (the black circles), the true VMISO result curve (the red solid line), and the VMISO with path-loss disparity but assuming independent $h_{0,0}$ and $g_{0,0}$ (the black 'x'-markers). We label the four curves with 'CA', 'CA-indp', 'VMISO', and 'VMISO-indp'. If we look at the VMISO curves indicated by the red solid lines in the three figures, the link asymmetry is very severe, because $p_{2X}$ varies from about 0.25 to 0.6 for all parameter variations.

is about 0.3 in the worst case scenario.

Fig. 7 displays the probability $p_{2X}$ indicated by the y-axis for the different distance ratio $d_0/r_s$ indicated by the x-axis, when $\alpha = 4$ and $L = 6$. In the figure, only the VMISO and VMISO-indp graphs, which correspond to the red solid line and black 'x'-markers, decrease, as the distance ratio $d_0/r_s$ increases, while the other two, CA and CA-indp, do not change. The decrease of the VMISO graphs happens because the path-loss disparity, which can be estimated by $\sigma^2$ in (6), becomes more severe, as $d_0/r_s$ increases. For the same reason, the VMISO group shows always higher $p_{2X}$ than the CA group that ignores the path-loss disparity by the random

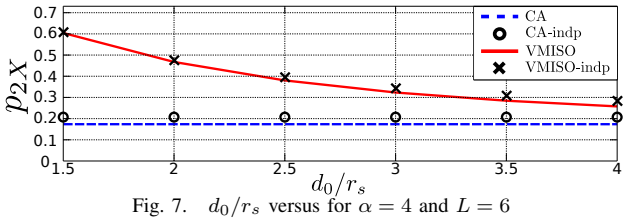


Fig. 7. $d_0/r_s$ versus for $\alpha = 4$ and $L = 6$

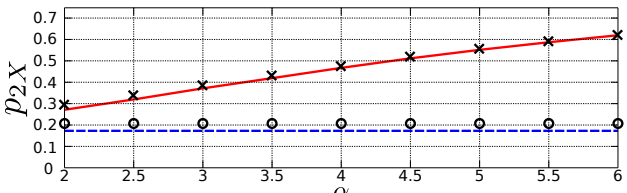


Fig. 8. $\alpha$ versus for $d_0/r_s = 2$ and $L = 6$

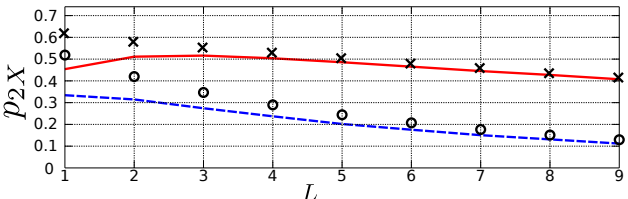


Fig. 9. $L$ versus for $d_0/r_s = 2$ and $\alpha = 4$

relay locations. Also, the gaps within the same groups (CA-to-CA-indp and VMISO-to-VMISO-indp) are very small, since the single common SISO link ($h_{0,0} = g_{0,0}$) has very little effect when $L = 6$.

Fig. 8 shows the impact of the path-loss exponent $\alpha$ on $p_{2X}$, when $d_0/r_s = 2$ and $L = 6$. The VMISO group graphs increase, as $\alpha$ increases, because the path losses of the different relays become more dissimilar, as $\alpha$ increases. We note that $\sigma^2$ in (6) is an increasing function of $\alpha$, which is consistent with the simulation results in Fig. 8. On the other hand, similarly to the previous results in Fig. 7, the other two results (CA and CA-indp) stay the same, because they are obtained by the co-located approximation.

In the last figure, Fig. 9, the four graphs show how the number of relays $L$ affects $p_{2X}$ with $d_0/r_s = 2$ and $\alpha = 4$. In contrast to Figs. 7 and 8, both the CA and VMISO groups have the identical trends: $p_{2X}$ decreases for $L \geq 2$, as $L$ increases. For small $L$, the two graphs in the same group (e.g., VMISO-to-VMISO-indp and CA-to-CA-indp) give a large gap, because the correlation $\rho$ is high for small $L$ as in Fig. 5. In general, since the correlation $\rho$ decreases for all the four cases corresponding to the four graphs, the link asymmetry must be reduced by diversity, as $L$ increases. In case of fully uncorrelated forward and reverse links, it is very unlikely to have extremely large or small power ratio $\eta$ because of diversity by using many nodes. For example, if plugging $M = N = L$ and $x = 0.5$ into (7), we can calculate the $p_{2X}$ of the CA-indp case in the figure as

$$p^*_{2X} = 2 \cdot F^*_\eta(1/2) = 3^{1-2L} \cdot \sum_{k=0}^{L-1} \binom{2L-1}{k} \cdot 2^{k+1}, \quad (9)$$

which is a monotonically decreasing function of $L$, because the first exponential term, $3^{1-2L}$, is dominant for a large $L$ compared to the remaining terms. Hence, $p_{2X}$ decreases, as $L$

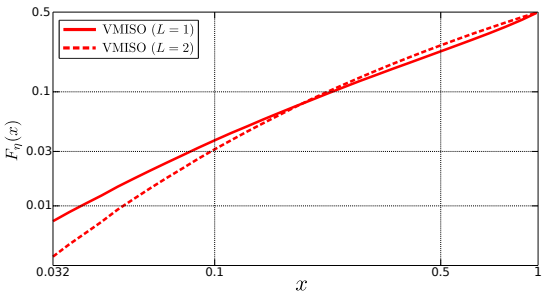


Fig. 10. $F_\eta(x)$ with $L = 1$ and 2 for $d_0/r_s = 2$ and $\alpha = 4$

increases in this case.

In contrast, the VMISO graph increases, as $L$ changes from one to two. However, it is just because we look at the tail probability that the two powers have more than 3dB gap, which is denoted by $p_{2X} = 2 \cdot F_\eta(0.5)$. If we look at the probability with even a higher power gap, for example $p_{10X} = 2 \cdot F_\eta(0.1)$, $L = 1$ gives a higher probability than $L = 2$. Fig. 10 shows the CDFs $F_\eta(x)$, which indicated by the y-axis, with $L = 1$ and 2 for $0.031 \leq \eta \leq 1$ as indicated by the x-axis, when $d_0/r_s = 2$ and $\alpha = 4$. In the figure, the curve with $L = 1$ is represented by the solid red line, while the $L = 2$ curve is indicated by the red dotted line. As shown in the figure, $L = 1$ gives lower $F_\eta(0.5) = 0.5 \cdot p_{2X}$ than $L = 2$, while the order is opposite for $F_\eta(0.1) = 0.5 \cdot p_{10X}$. Therefore, we can say the link asymmetry level decreases by the influence of the diversity, as $L$ increases, which also makes $\rho$ decrease.

## V. Conclusion

In this paper, we study the link asymmetry between the forward and reverse VMISO links, where physically separated nodes in one cluster transmit together to a single receiver node in the other cluster. We present the two main causes of the VMISO link asymmetry, which the conventional SISO links do not experience: the exclusive signal reception of the cluster head and the path-loss disparity. We present the level of the VMISO link asymmetry by two measures: the power correlation $\rho$ and the power ratio $\eta$ of the forward and reverse links. Moreover, we show the relationship between the VMISO link asymmetry with the system parameters such as $d_0/r_s$, $\alpha$, and $L$. Also, the simulation results on $p_{2X}$, which tells the probability that two powers have more than 3dB difference, indicate that VMISO link asymmetry can be much more severe than SISO links, which cannot be expected by the co-located approximation. Hence, this paper should sensitize designers of CT-based higher-layer protocols that require bidirectional links to the situation that successful decoding of a packet in the forward direction is little guarantee that a similar packet will be decoded in the reverse direction. Possible future work includes a detailed analysis of the impact of the VMISO link asymmetry on network capacity and throughput in multi-hop networks.

## Acknowledgment

The authors gratefully acknowledge partial support for this research from the National Science Foundation, grant number CNS-1017984.

## References

[1] A. Sendonaris, E. Erkip, and B. Aazhang, "User cooperation diversity. part i. system description," *IEEE Trans. Commun.*, vol. 51, no. 11, pp. 1927 – 1938, Nov. 2003.

[2] J. Laneman, D. Tse, and G. Wornell, "Cooperative diversity in wireless networks: Efficient protocols and outage behavior," *IEEE Trans. Inf. Theory*, vol. 50, no. 12, pp. 3062–3080, Dec. 2004.

[3] B. Sirkeci-Mergen, A. Scaglione, and G. Mergen, "Asymptotic analysis of multistage cooperative broadcast in wireless networks," *IEEE Trans. Inf. Theory*, vol. 52, no. 6, pp. 2531–2550, June 2006.

[4] L. Thanayankizil, A. Kailas, and M. A. Ingram, "Routing for wireless sensor networks with an opportunistic large array (OLA) physical layer," *Ad Hoc & Sensor Wireless Networks*, vol. 8, no. 1-2, pp. 79–117, 2009.

[5] J. Yackoski, L. Zhang, C.-C. Shen, L. Cimini, and B. Gui, "Networking with cooperative communications: Holistic design and realistic evaluation," *Commun. Magazine, IEEE*, vol. 47, no. 8, pp. 113–119, Aug. 2009.

[6] T. Halford, K. Chugg, and A. Polydoros, "Barrage relay networks: System and protocol design," *in Proc. IEEE PIMRC*, pp. 1133–1138, Sept. 2010.

[7] Z. Zhou, S. Zhou, S. Cui, and J.-H. Cui, "Energy-efficient cooperative communication in a clustered wireless sensor network," *IEEE Trans. Vehicular Tech.*, vol. 57, no. 6, pp. 3618 –3628, Nov. 2008.

[8] G. Jakllari, S. V. Krishnamurthy, M. Faloutsos, and P. V. Krishnamurthy, "On broadcasting with cooperative diversity in multi-hop wireless networks," *IEEE J. on Sel. Areas in Commun.*, vol. 25, no. 2, pp. 484–496, Feb. 2007.

[9] A. Aksu and O. Ercetin, "Reliable multi-hop routing with cooperative transmissions in energy-constrained networks," *IEEE Trans. Wireless Commun.*, vol. 7, no. 8, pp. 2861 –2865, Aug. 2008.

[10] G. Jakllari, S. V. Krishnamurthy, M. Faloutsos, P. V. Krishnamurthy, and O. Ercetin, "A cross-layer framework for exploiting virtual MISO links in mobile ad hoc networks," *IEEE Trans. Mobile Computing*, vol. 6, no. 6, pp. 579 –594, June 2007.

[11] S. Lakshmanan and R. Sivakumar, "Diversity routing for multi-hop wireless networks with cooperative transmissions," *in Proc. IEEE SECON*, pp. 1 –9, June 2009.

[12] J. W. Jung and M. A. Ingram, "Residual-energy activated cooperative transmission (REACT) to avoid the energy hole," *in Proc. IEEE ICC*, June 2010.

[13] A. Scaglione, D. Goeckel, and J. Laneman, "Cooperative communications in mobile ad hoc networks," *IEEE Sig. Proc. Magazine*, vol. 23, no. 5, pp. 18 – 29, Sept. 2006.

[14] V. Ramasubramanian and D. Mosse, "BRA: A bidirectional routing abstraction for asymmetric mobile ad hoc networks," *IEEE/ACM Trans. Networking*, vol. 16, no. 1, pp. 116–129, 2008.

[15] V. Ramasubramanian, R. Chandra, and D. Mosse, "Providing a bidirectional abstraction for unidirectional ad hoc networks," *in Proc. IEEE INFOCOM*, vol. 3, pp. 1258 – 1267 vol.3, 2002.

[16] "IEEE Standard for Wireless LAN Medium Access Control (MAC) and Physical Layer (PHY) Specifications," Nov.

[17] G. Caire and S. Shamai, "On the capacity of some channels with channel state information," *IEEE Trans. Info Theory*, vol. 45, no. 6, pp. 2007–2019, 1999.

[18] S. Cui, A. Goldsmith, and A. Bahai, "Energy-efficiency of mimo and cooperative mimo techniques in sensor networks," *IEEE J. on Sel. Areas in Commun.*, vol. 22, no. 6, pp. 1089–1098, 2004.

[19] N. C. Beaulieu and J. Hu, "A closed-form expression for the outage probability of decode-and-forward relaying in dissimilar rayleigh fading channels," *IEEE Commun. Letters,*, vol. 10, no. 12, pp. 813 –815, december 2006.

[20] H. Jung, Y. Chang, and M. A. Ingram, "Experimental range extension of concurrent cooperative transmission in indoor environments at 2.4GHz," *in Proc. IEEE MILCOM*, Oct. 2010.

[21] S. Hassan and M. A. Ingram, "A quasi-stationary markov chain model of a cooperative multi-hop linear network," *IEEE Trans. Wireless Commun.*, vol. 10, no. 7, pp. 2306 –2315, July 2011.

[22] H. Jung and M. A. Ingram, "SNR penalty from the path-loss disparity in virtual multiple-input-single-output (VMISO) link," *in Proc. IEEE ICC*, June 2013.

[23] M. K. Simon and M.-S. Alouini, "On the difference of two chi-square variates with application to outage probability computation," *IEEE Trans. Commun.*, vol. 49, no. 11, pp. 1946–1954, 2001.